# AN EXPERIMENTAL FRACTURE-MECHANISM MAP FOR THORIA DISPERSION-STRENGTHENED NICKEL

C. Gandhi*, D. M. R. Taplin* and M. F. Ashby**

## INTRODUCTION

DS-Nickel is an alloy with an exceptionally stable microstructure, developed, and now used, as a high-temperature material. Its microstructure consists of small grains of almost pure nickel, elongated in the direction in which the material was worked. These long grains are stabilized and the material strengthened by the presence of a fine dispersion of $ThO_2$ - about 2 vol % in the alloy we studied. In characterizing this material, it is important to examine the various mechanisms by which it may fracture, with the ultimate aim of developing constitutive laws for each of them. One way to approach this problem is to construct a *fracture mechanism diagram* (Ashby [1, 2]) for the material: it is a diagram with stress as one axis and temperature as the other, showing the range of dominance of each mechanism of failure. In the present paper we describe creep tests and fractography, carried out on DS-Nickel, which allows us to identify mechanisms of failure. These measurements have been combined with data from the literature to construct a fracture mechanism map.

## EXPERIMENTAL

Nickel containing a dispersion of 1.93 vol % of thoria (supplied by Sherritt-Gordon Mines Ltd., Canada) was annealed for 12 hours at 1473 K in argon and machined to tensile-creep specimens 4.4 mm in diameter, with a gauge length of 16 mm. These were polished and then tested to failure in a vacuum, under a constant load, at three temperatures: 583, 673 and 873 K. The creep curve and the time-to-fracture (between 60 and $10^7$ secs) were recorded and the fracture surface examined by optical and scanning electron microscopy.

## RESULTS

### Microstructure

The annealed material had structure very like that described by Wilcox and Clauer [3, 4, 5]: elongated grains, about 1 μm wide and 10 μm long, containing a dispersion of $ThO_2$ with a particle diameter of about 400 Å.

* Department of Mechanical Engineering, University of Waterloo, Waterloo, Ontario, Canada
** University Engineering Department, University of Cambridge, Cambridge, England

### Creep Measurements

The creep and fracture times are plotted in Figure 1, together with those of Wilcox and Clauer [5]. At low temperatures, or at high stresses, the strain-rates and times-to-fracture vary rapidly with stress: if the curves of Figure 1 are described by a power law, then, in this regime,

$$\frac{1}{t_f} \alpha \dot{\varepsilon}_{ss} \alpha \sigma^n \qquad n > 30 \ . \tag{1}$$

At higher temperatures, and at lower stresses, the deformation is more like classical power-law creep, though the power is still a large one:

$$\frac{1}{t_f} \alpha \dot{\varepsilon}_{ss} \alpha \sigma^n \qquad n \sim 8 \ . \tag{2}$$

These observations are consistent with those of Wilcox and Clauer [5] on extruded and annealed Ni-2% $ThO_2$.

### Fractography

Optical microscopy of all our fractured specimens, longitudinally sectioned, showed voids throughout the gauge length; evidently they nucleated with great ease (see, for example, the work of Olsen et al [6]). But the way they subsequently grow, depends on temperature, giving - in the case of our specimens - different fracture surface topologies at different temperatures.

At the lowest temperature (583 K) all the specimens we tested failed in a ductile transgranular manner. Figure 2 is an example. This specimen showed 22% elongation and 80% reduction in area (Figure 2a). Scanning micrographs (Figure 2b) show a typically ductile "double cup" topography: in the central region, the fracture surface shows equiaxial cusps; at the edge (the final zone of fracture, in which the parting occurs by a void-sheet mechanism) the cusps are hyperbolic and elongated. At a higher magnification (Figure 2c) the void surfaces are rough, suggesting slip lines have intersected them and implying that the voids grew by plastic flow of the surrounding nickel. At this temperature, the stress DS-Nickel behaves almost as it does at room temperature - it flows only when its yield strength is exceeded. We will call this fracture "ductile transgranular fracture".

At the intermediate temperature (673 K) too, all our specimens failed in a ductile transgranular manner. Here, the material creeps, but with a very high stress exponent ($n > 30$). The ductility was still large, but decreased slightly with decreasing stress. Because the material is now creeping we shall call this "transgranular creep fracture".

At the highest temperature (873 K), the specimens tested at the higher stresses (when $n > 30$) failed in a transgranular way, but as the stress was decreased, not only did the creep exponent fall (to about 8) but the fracture changed to a partly or totally intergranular one. The sample tested at 177 MPa is at this transition and shows two types of fracture (Figure 3a). The outer anulus (Figure 3b) was the last part to fail; it looks much like transgranular creep fracture described above. But the central position is intergranular, showing pulled-out grains, the surfaces of which appear puckered or cusped because they are covered by small voids -





smaller than those in Figure 2 - which are linked to give a fracture path (Figure 3c). These grain-boundary voids seem to be less rough than those of Figure 2, suggesting that, if plasticity contributed to their growth, that it was more homogeneous than at the lower temperature, perhaps because the matrix can now creep freely. This intergranular fracture resembles in every way the fracture of Ni-2% $ThO_2$ observed by Wilcox and Clauer [3], at between 1073 and 1373 K. We shall call this "intergranular creep fracture", although, because of the elongated grain structure of DS-Nickel, its appearance is unlike most such fractures.

## DISCUSSION

### Construction of a Fracture Mechanism Map

The data is plotted in another way in Figure 4. Its axes are *tensile stress normalized by Young's Modulus* ($\sigma_1/E$) and, *homologous temperature* ($T/T_m$). A point on the figure shows the stress and temperature at which a given test was carried out, and is labelled, where it is appropriate to do so, with the logarithm, to the base 10, of the time-to-fracture in seconds. The figure includes not just our own data, but all the published, fracture data we could find for nickel containing about 2% $ThO_2$, obtained in creep tests (points with numbers associated with them) and in tensile tests (points without numbers).

The mechanism by which our samples failed has been discussed already. A mechanism can be assigned to many of the other points too - most of the sources listed on Figure 4 give enough information to allow this. We have used this information to draw one of the *field boundaries* on the map: that separating transgranular from intergranular fracture. The other boundary separates the region creep from the yield region - it is the mechanism of plastic flow, not of fracture, which changes as we cross this boundary but since the constitutive law for fracture depends on both, it is important to know where the boundary lies. In this way, we have divided the map into three fields: *ductile transgranular fracture*, typical of behaviour near room temperature; *transgranular creep fracture*, typical of fast creep tests; and *intergranular creep fracture*, typical of slow creep tests. Each is characterized by a different constitutive law for fracture.

Our experimental observations, and those in the literature, do not permit us to subdivide the map further - yet further subdivisions must certainly exist. At very high temperatures, for instance, we might expect a regime in which holes grow on boundaries in a purely diffusional way. And close to the melting point, recrystallization may accompany plastic flow, again leading to a new field on the map. Neither has been observed in DS-Nickel, probably because there have been no experiments in these ranges of stress and temperature.

### The Micromechanisms of Fracture

An upper limit to the strength of DS-Nickel is set by its *ideal tensile strength*. If this stress - about E/6 [7] - were applied to the solid, it would fail simply because the strength of the interatomic bounds has been exceeded.

Few solids exhibit such high strengths. At low temperatures b.c.c. and h.c.p. metals, and virtually all ceramics, fail by *cleavage* at a stress

often orders of magnitude less than the ideal strength.

The plasticity of f.c.c. metals prevents their cleaving, but at low temperatures they commonly fail by an alternative mechanism (exhibited also by the b.c.c. and h.c.p. metals): at stresses well below E/5, holes nucleated usually at inclusions, within the deforming solid; these grow by plastic flow until they link, leading to *ductile transgranular fracture*. The interfacial strength of thoria in nickel has been measured [6] although it probably varies from batch to batch, this value of 210 MPa must be broadly typical. As Figure 4 shows, the external stress in most of the creep and tensile tests exceeds this, so that - even without allowing for the stress concentrating effects of particles - holes can nucleate at $ThO_2$ particles as soon as the sample is loaded.

Further strain is required to cause the holes to grow and link. Although this process is incompletely understood, it appears that the growth strain $\varepsilon_g$ is determined more by the volume fraction of particles than by anything else. Brown and Embury [8] show, for example, that data for copper correlates well with

$$\varepsilon_g = A \ln \frac{1}{\sqrt{f}} . \qquad (3)$$

This model can be adapted to deal with grain boundary fracture also [2]: if the area-fraction $f_b$ of particles on grain boundaries greatly exceeds the average volume fraction $f_v$ in the grains, then - although the fracture is ductile - the fracture path tends to be a grain-boundary one; such fractures occur if DS-Nickel is pulled in the transverse direction (at right-angles to the direction of elongation of the grains). But when it is pulled in the longitudinal direction, most boundaries lie parallel to the maximum principal stress, the holes on them do not link, and the fracture path remains transgranular. Only when the temperature is high enough that grain boundary sliding becomes rapid is there a mechanism for linking the boundary cavities, giving a *creep-controlled intergranular fracture*. Both in our experiments and in those of Wilcox and Clauer [5] this appears to be the dominant mechanism of failure at high temperatures and low stresses. In the creep regime cavity-linkage may be postponed by the rate-sensitivity of the material [9]. A phenomenological way of modifying equation (1) to deal with this is discussed elsewhere [2]. Hancock [10] has also recently discussed the problem of plasticity-controlled cavity growth and linkage.

There remains the possibility of a *diffusion-controlled intergranular fracture* [11 - 14]. At high temperatures, voids on grain boundaries under tension should grow by diffusion - either by grain-boundary or by lattice diffusion - whichever is faster. The elongated grain shape in DS-Nickel tends to inhibit this mechanism; when loaded in the longitudinal direction, few boundaries are in tension. And the picture of diffusion-controlled growth described in these papers is probably too simple: recent work suggests a number of modifications, each applicable in a particular stress regime [e.g., 10]. The conclusion is that several intergranular fracture mechanisms exist, and that, as our understanding of them increases, we should be able to divide this field into a number of sub-fields. It is important to do so, since both in the extrapolation of creep fracture data, and in selecting a constitutive law for design, it is essential to know the dominant mechanism, or sub-mechanism of fracture.





ACKNOWLEDGEMENTS

Assistance from S. Kadela with regard to the experimental work, is acknowledged with particular gratitude. The financial assistance for this research work comes from the National Research Council of Canada and it is acknowledged with pleasure.

REFERENCES

1. ASHBY, M. F., "Progress in the Development of Fracture Mechanism Maps", Fracture 1977, D. M. R. Taplin, Editor, University of Waterloo Press, Canada, 1977.
2. ASHBY, M. F., to appear in Acta Met., 1977.
3. WILCOX, B. A. and CLAUER, A. H., Trans. AIME, 233, 1965, 253.
4. WILCOX, B. A. and CLAUER, A. H., Trans. AIME, 233, 1965, 253.
5. WILCOX, B. A. and CLAUER, A. H., Acta Met., 20, 1972, 743.
6. OLSEN, R. J., JUDD, G. and ANSELL, G. S., Met. Trans., 2, 1971, 1353.
7. KELLY, A., "Strong Solids", Cambridge University Press, 1966.
8. BROWN, L. M. and EMBURY, J. D., "Microstructure and Design of Alloys", Inst. Met., 1, 1973, 164.
9. SAGAT, S. and TAPLIN, D. M. R., Acta Met., 24, 1976, 307.
10. HANCOCK, J. W., Met. Sci., 10, 1976, 319.
11. HULL, D. and RIMMER, D. E., Phil. Mag., 4, 1959, 673.
12. RATCLIFFE, R. T. and GREENWOOD, G. W., Phil. Mag., 12 1965, 59.
13. SPEIGHT, M. V. and HARRIS, J. E., Met. Sci. J., 1, 1967, 83.
14. RAJ, R. and ASHBY, M. F., Acta Met., 23, 1975, 653.

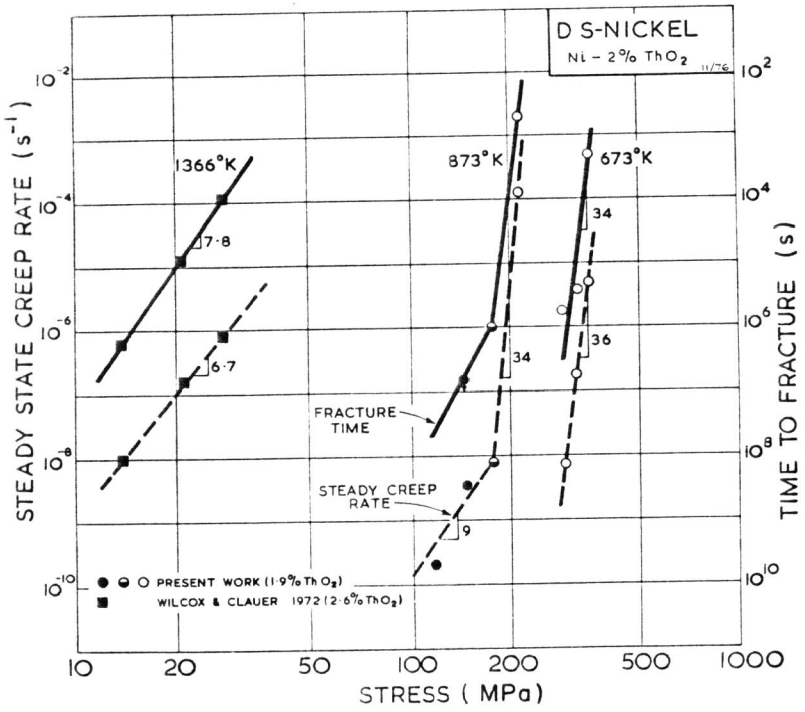


Figure 1 The Steady-State Creep Rate ($\dot{\varepsilon}_{SS}$, broken lines) and the Reciprocal of the Time-to-Fracture ($1/t_f$, full lines) Plotted, on Logarithmic Scales. The Similarities in the Slopes and Kinks in the Two Sets of Curves Suggest that Plasticity or Power-Law Creep Determine the Life





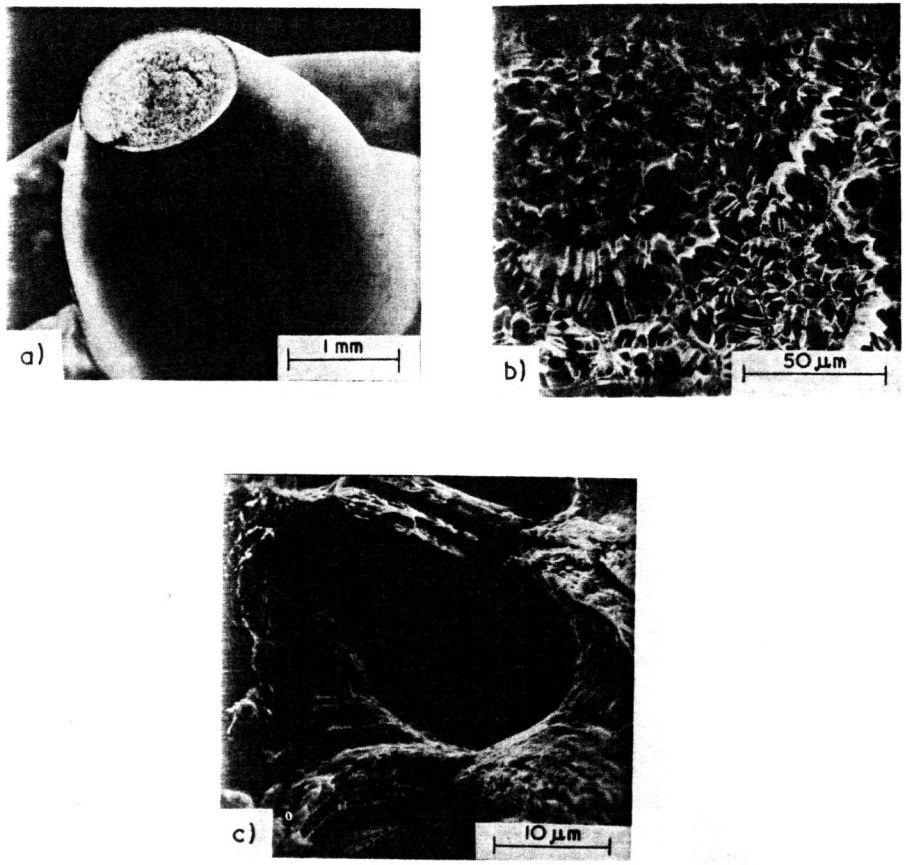


Figure 2 Features of Ductile Fracture for a Specimen Tested at 583 K Under 471 MPa

(a) Pronounced Neck Formation
(b) Scanning Electron Micrograph Showing the Presence of Numerous Holes Associated with Particles
(c) Details of a Void Showing Much Plasticity

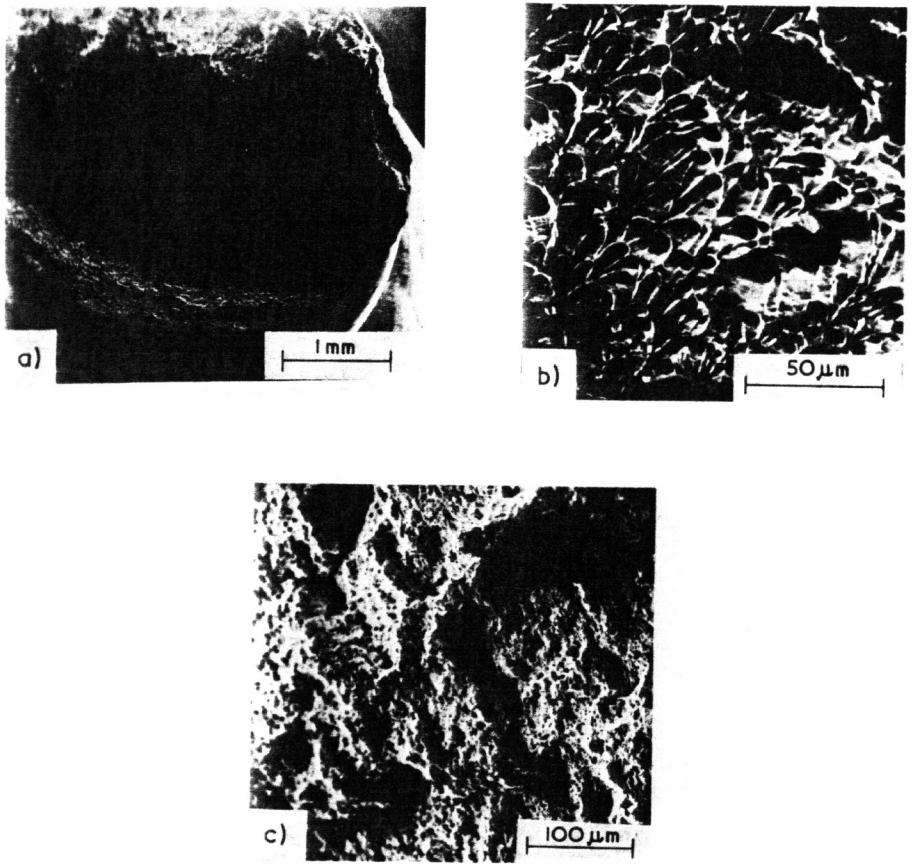


Figure 3 Features of the Fracture of a Specimen Tested at 873 K Under 177 MPa

(a) Fracture Surface Showing Two Fields: Shear Lip (outer region) and Brittle Surface (central region)
(b) Scanning Electron Micrograph Showing Elongated Holes in the Shear Lip
(c) Scanning Electron Micrograph Showing the Grain Facet and Grain Boundary Cracking. Notice that the Cavities on the Boundaries are Small and Shallow





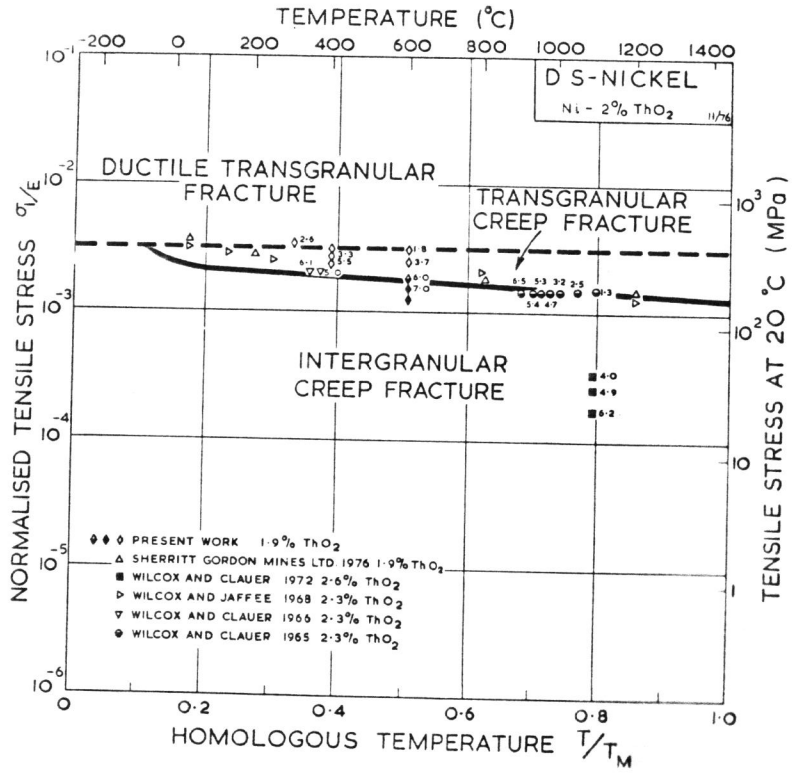


Figure 4 Experimental Fracture Mechanism Map for DS-Nickel Showing Three Fields: Ductile Fracture at Low Temperatures, Transgranular and Intergranular Fracture Fields at Elevated Temperatures. The Points Show Individual Tests and, in the Case of Creep Tests, are Labelled with the $\log_{10}$ of the Time-to-Fracture in Seconds